Int J Heat Mass Transfer Vol 33, No 11 pp 2565–2578 1990
Printed in Great Britain

0017-9310/90 $3 00 + 0 00

Effect of Prandtl number on buoyancy-induced transport processes with and without solidification

WEI SHYY and MING-HSIUNG CHEN
Department of Aerospace Engineering, Mechanics and Engineering Science, University of Florida, Gainesville, FL 32611, U S A

(*Received* 25 *October* 1989 *and in final form* 22 *January* 1990)

Abstract—In studying the transport processes with solidification, various materials such as aqueous solutions, which are of high Prandtl number (*Pr*), have been used to help understand the solidification characteristics of silicon or metal based materials, which are of low *Pr*. Influences of *Pr* on the buoyancy-induced transport phenomena are investigated through two-dimensional steady-state computations for flow in a square enclosure at two different vertical wall temperatures, both with and without solidification. With a constant Rayleigh number (*Ra*), the momentum and heat transport characteristics are very insensitive to *Pr* if $Pr > 1$, regardless of whether phase change appears or not. The *Pr* effect becomes more noticeable as it is progressively reduced from one. With respect to phase change, for cases with no solidification, *Pr* effects on all aspects of the transport process increase with *Ra*. With solidification, more vigorous convection induced by higher *Ra*, which coupled with the Stefan number effects, result in stronger *Pr* influence on maximum streamfunction and Nusselt number, but not on global enthalpy patterns. It is also found that features such as morphology of phase boundaries may be more sensitive to *Pr* variations than momentum and heat transport are.

1. INTRODUCTION

IT IS WELL established that fluid flow phenomena play a major role in affecting the large-scale grain structure and the macrosegregation of solidifying materials [1–6]. The interaction of fluid flow with a solidifying medium is a complex problem with multiple characteristics, notably the convection effect both in the bulk of the melt and in the interdendritic region. The considerable practical importance of macrosegregation in affecting the quality of solidifying materials, including the ones that need high and well-controlled performance such as semiconductors used in computer hardware and superalloys used in aerospace vehicles, has stimulated extensive research into this field.

Heat and fluid flow phenomena associated with laminar buoyancy-induced natural convection relevant to material processing have been extensively studied based on the fundamental conservation laws of the mass continuity, momentum, energy, and species concentration. In refs. [7–10], direct theory/data comparisons have also been presented. In those works, various fluids have been used, including the aqueous solution of ammonium chloride (NH_4Cl–H_2O) [7–9], aqueous solution of sodium carbonate (Na_2CO_3–H_2O) [10], water [8], and glycerine [8]. In a related experimental work, Kamotani *et al.* [11] used water and silicone oils to study natural convection without phase change. These materials are attractive because their thermophysical property data are relatively well established, and their low entropy of fusion makes them solidify qualitatively like metallic alloys to be investigated. Furthermore, for a system such as the aqueous solution of ammonium chloride, the transparent nature of the solution and the translucency of ammonium chloride dendrites allow ready visual examination of the solidification process.

The physical properties of the above-mentioned fluids are not close to the materials commonly used in the semiconductor or metallic alloy applications. The Prandtl numbers (*Pr*) of the aqueous ammonium chloride, aqueous sodium carbonate, water, and glycerine used in the aforementioned experiments are, respectively, 9 025 [9], 6 [10], 6.44 [8], and $8\,356 \times 10^3$ [8]. The Prandtl number of the silicone oil used by Kamotani *et al* [11] ranged from 3.65×10^2 to $1\,93 \times 10^4$. However, the Prandtl numbers relevant to the melt crystal growth of both the semiconductor and metallic alloy materials are small, ranging from 10^{-2} to 10^{-1}. For example, the Prandtl number for gallium-doped germanium and silicon–germanium crystal growth was reported to be 7×10^{-3} [6]. The Prandtl number of pure gallium studied by Gau and Viskanta [12] is 0 0208. It is also known that the titanium based superalloys have a Prandtl number of about 10^{-1}. The Prandtl number of the aluminum–tin alloy, studied numerically by Bergman and Keller [13], is $1\,49 \times 10^{-2}$.

As surveyed by Gebhart *et al* [14], various empirical correlations have been proposed in the literature to quantify the effect of Prandtl number on the heat transfer characteristics. However, they were all limited to single phase fluids and are not necessarily consistent among one another. Here, we study the effect of

NOMENCLATURE

C_p	specific heat	β	thermal expansion coefficient of liquid
D	length of the domain	λ	porosity
g	gravitational acceleration	ν	kinematic viscosity
Gr	Grashof number		
L	latent heat of phase change		
p	pressure	Subscripts	
Pr	Prandtl number	C	cold
Ra	Rayleigh number	H	hot
St	Stefan number	ℓ	liquidus phase
T	temperature	s	solidus phase
x, y	Cartesian coordinates		
Greek symbols		Other symbol	
α	thermal diffusivity of liquid	$\bar{}$	dimensional quantity

Prandtl number on the transport process of fluid with and without solidification It is hoped that with more understanding of the effect of the Prandtl number, cross references of transport characteristics can be drawn with more confidence among different materials

2. NUMERICAL FORMULATION

We have utilized the two-dimensional Navier–Stokes equations, including the mass continuity, momentum, and energy equations, with the following treatments

(1) Boussinesq approximation for the density variation,

(2) Darcy law modeling of the effect of the mushy region between solid and liquid,

(3) enthalpy formulation instead of temperature formulation for the energy equation

For problems with phase change, the enthalpy formulation alleviates the need for explicitly tracking the phase boundaries, but introduces extra source terms arising from the release of latent heat which can make the computation more difficult to converge [15, 16]. We have developed the numerical methods capable of accounting for the above described physical models in the framework of the general curvilinear coordinates [16]

In terms of the non-dimensionalization procedure, the length of the whole domain, $\bar{D}$, thermal diffusivity of the liquid phase, $\bar{\alpha}$, specific heat, $\bar{C}_p$, and temperature differences between the right (hot) and left (cold) walls, $(\bar{T}_H - \bar{T}_C)$, are used as the reference physical quantities Hence, the reference velocity and enthalpy scales are, respectively, $\bar{\alpha}/\bar{D}$ and $C_p(\bar{T}_H - \bar{T}_C)$ The governing equations have been presented in ref. [16] and will not be repeated here

The Rayleigh number is defined, with the overbar designating the dimensional quantities, as

$$Ra = \frac{\bar{g}\bar{\beta}(\bar{T}_H - \bar{T}_C)\bar{D}^3}{\bar{\nu}\bar{\alpha}} \tag{1}$$

and the Prandtl number is

$$Pr = \frac{\bar{\nu}}{\bar{\alpha}} \tag{2}$$

where $\bar{\nu}$ and $\bar{\alpha}$ are, respectively, kinematic viscosity and thermal diffusivity, $\bar{g}$ the gravitational acceleration, $\bar{\beta}$ the thermal expansion coefficient of liquid, and $\bar{D}$ the dimension of the square domain By combining the Rayleigh and Prandtl numbers, the Grashof number, Gr, emerges as

$$Gr = \frac{Ra}{Pr} \tag{3}$$

The dimensionless parameter associated with the phase change is the Stefan number, defined as

$$St = \frac{\bar{C}_p(\bar{T}_H - \bar{T}_C)}{\bar{L}} \tag{4}$$

where $\bar{L}$, $\bar{C}_p$, and $\bar{T}_H$ and $\bar{T}_C$ are, respectively, latent heat of the liquid, specific heat of the material, and the boundary values of the temperature field associated with the hot and cold walls

The solution methodology [17, 18] employs a semi-implicit iterative algorithm capable of solving the coupled equations in non-orthogonal curvilinear coordinates Along with the coordinate transformation, the finite volume formulation has been adopted in order to accurately honor the physical conservation laws A combined use of the Cartesian velocity components and contravariant velocity components is derived in the numerical algorithm In the momentum equations the Cartesian velocity components are treated as the primary variables In the continuity (pressure correction) equation the con-

travariant velocity components are first updated and then the D'yakonov iteration is used to yield the corresponding values between the contravariant and Cartesian velocity components in an efficient manner

The staggered grid system [17] is employed to store the dependent variables The second-order central difference schemes are used to discretize all the terms in the governing equations except the convection terms which are approximated by the second-order upwind scheme.

3 RESULTS AND DISCUSSION

Both the single- and multiple-phase fluids have been considered The steady-state solutions of the flow within a two-dimensional square enclosure have been computed for a wide range of Prandtl numbers, from 1.49×10^{-2} to 10^3 The Rayleigh number is varied from 10^4 to 10^5 The corresponding Grashof number is from 10 to 10^2 for $Pr = 10^3$, and from 6.71×10^5 to 6.71×10^6 for $Pr = 1.49 \times 10^{-2}$. The boundary conditions used are shown in Fig 1 The no-slip boundary condition is prescribed for the velocity variables along all sides, and the constant wall temperature on two vertical boundaries, i e $T_H = 1$ ($\phi_H = 1$) and $T_C = 0$ ($\phi_C = 0$), and adiabatic (zero normal gradient) condition on both the top and bottom walls For the fluid undergoing a solidification process, the minimum liquidus temperature and the maximum solidus temperature are 0 6 and 0.4, respectively, to define the boundaries of the mushy zone. This corresponds to a Stefan number of 0 2 An initial grid system consisting of 81×81 nodal points was used first to yield the solution An adaptive grid method [19] was then used to enhance the numerical accuracy and convergence rates, especially for low Pr fluids As demonstrated in refs [16, 19, 20], for the present type of problems, even with an idealized geometry such as a square, the adaptive grid method can be useful. All the quantities to be presented in the following sections are based on the dimensionless quantities

3 1 *Without solidification*

3 1 1. $Ra = 10^4$ Figure 2 compares the streamfunction contours of a single-phase fluid computed for $Ra = 10^4$ and four different Prandtl numbers. While a monotonic trend can be observed for the convection strength with respect to the Prandtl number, the correlation between them is not linear. Very small changes occur with Pr being reduced from 10^3 to 1, the difference of the maximum streamfunctions between the two cases is 1 5%.

As the Prandtl number is further lowered, the rate of decrease of convection strength expedites The maximum streamfunctions differ by 4.6% with Pr decreasing from 10^3 to 10^{-1}, and 10.2% from $Pr = 10^3$ to 1.49×10^{-2} Hence, the overall impact of Prandtl number on convection is very modest with five orders of variation of Pr causing only less than 11% differences of convection strength. Qualitatively, the shapes of the streamlines change from a rectangular geometry of high Pr to a circular geometry of low Pr

It is noted that the Grashof number of the $Pr = 10^3$ case is only 10 for $Ra = 10^4$ However, with the same Ra, the present results demonstrate that the transport process of $Pr = 10^3$ is not dominated more by the conduction than that of $Pr = 1.49 \times 10^{-2}$, the corresponding Gr of which is 6.71×10^5 Hence the

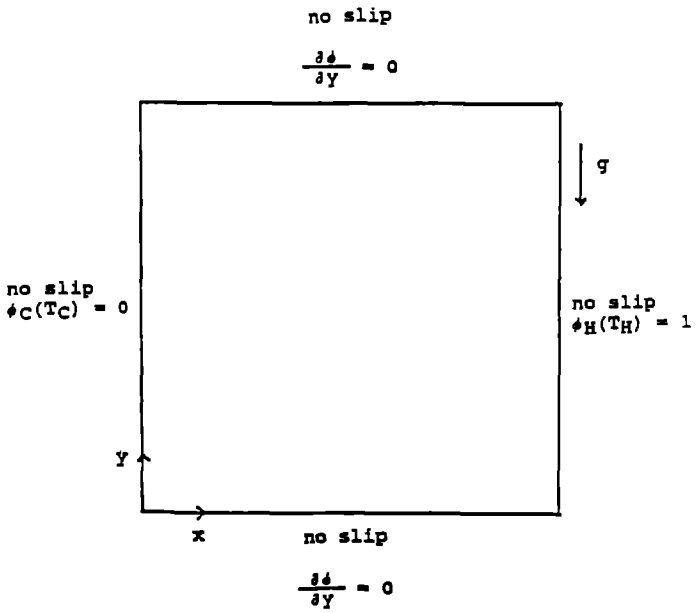

FIG 1 Schematic of geometry and boundary conditions

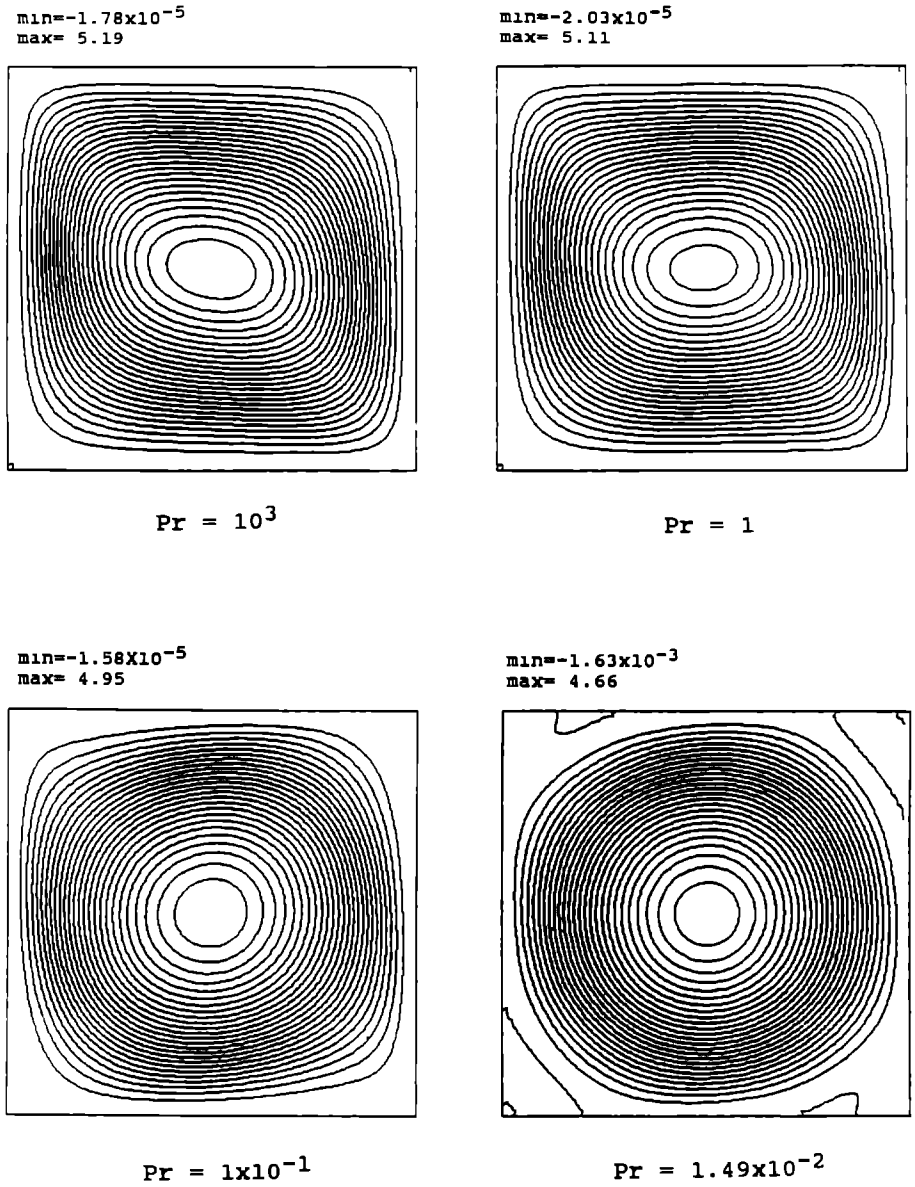

FIG. 2 Effect of Prandtl numbers on streamfunction with $Ra = 10^4$ and no phase change

Rayleigh number is a more reliable indicator of the relative importance of the convection effect

Figure 3 shows the corresponding enthalpy contours of the solutions with four different Prandtl numbers Very close resemblances are again observed for all cases The contours of a high Pr fluid show more concentration in the top left and bottom right corners The temperature profiles along the bottom wall are presented in Fig 4 for the four cases Similar to the streamfunction comparison, the profiles of $Pr = 10^3$ and 1 are very close to each other Further lowering the Prandtl number causes the temperature profiles to show more differences Hence, both the velocity and enthalpy fields show that the Prandtl number does not have a strong effect on the solutions with the same Ra

A qualitative explanation of this phenomenon can be delineated as follows At constant Ra but different Pr, the thermal diffusivity and kinematic viscosity of the fluid must simultaneously vary in the opposite directions and at the same rate. Hence, for instance, as Pr increases, the Grashof number decreases, indicating that *if* the temperature field remains unchanged, the convection effects weaken due to higher values of kinematic viscosity A higher Pr also means lower thermal diffusivity, which results in a more concentrated distribution of the temperature field *if* the convection field remains unchanged In

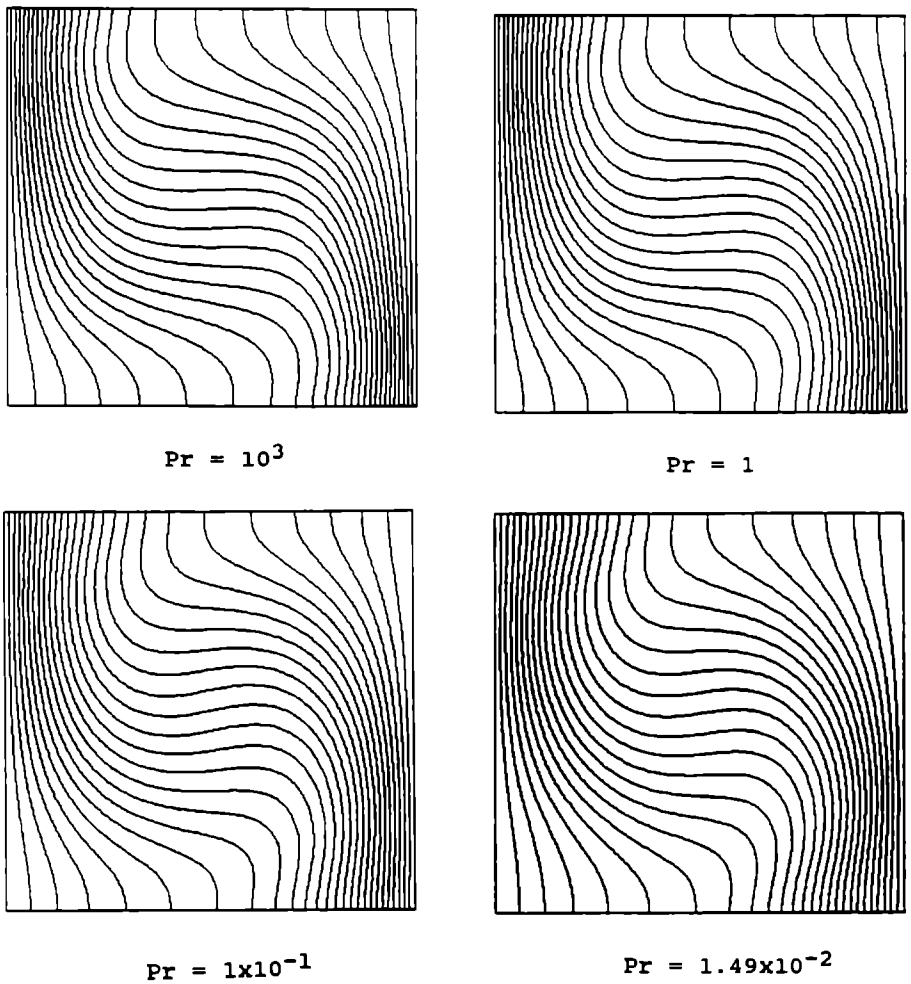

FIG 3 Effect of Prandtl numbers on enthalpy contours with $Ra = 10^4$ and no phase change

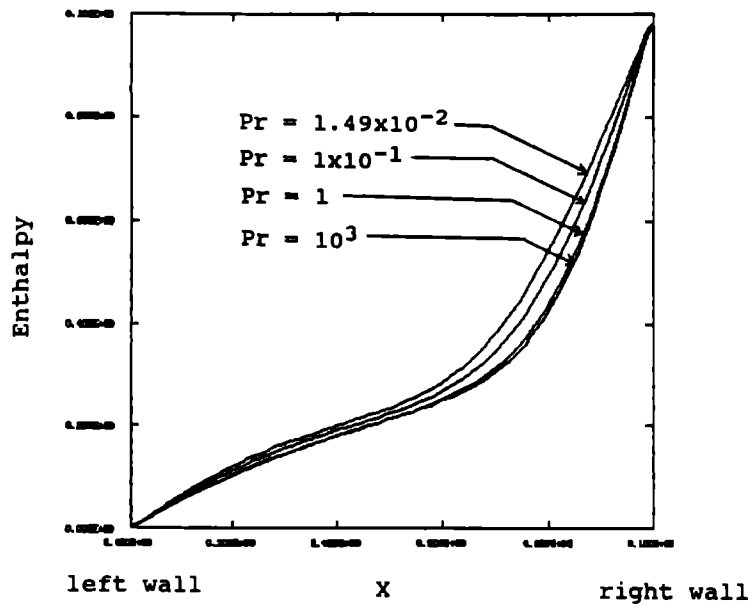

FIG 4 Effect of Prandtl numbers on enthalpy profiles along bottom wall with $Ra = 10^4$ and no phase change

balance, the weakened tendency of the convection effect and the strengthened tendency of the thermal buoyancy effect can largely compensate each other, causing the overall transport process to be insensitive to the variation of Pr

3 1 2 $Ra = 10^5$ Figures 5–7 depict, respectively, the streamfunction contours, enthalpy contours, and enthalpy profiles along the bottom wall, of $Ra = 10^5$ and four different Prandtl numbers Compared to the cases at $Ra = 10^4$, the trend is qualitatively similar but not quantitatively identical For $Ra = 10^5$, there is 10% difference between the maximum streamfunctions with $Pr = 10^3$ and 1, which is larger than that for $Ra = 10^4$ (1 5%). From $Pr = 10^3$ to 10^{-1}, the difference is 29 8% for $Ra = 10^5$ and only 4 6% for $Ra = 10^4$ A similar statement can also be made for $Pr = 1\ 49 \times 10^{-2}$ Furthermore, at $Ra = 10^5$ the convection pattern of $Pr = 1\ 49 \times 10^{-2}$ exhibits multiple secondary and tertiary cells in the corner regions which occupy noticeable areas, the contours in the corner regions represent the boundaries between adjacent convection cells This feature is qualitatively similar to that observed by Gresho and Upson [21] Hence we observe a stronger impact of Prandtl number on the convection strength as the Rayleigh number becomes higher The enthalpy contours also depict similar responses to Pr with both Rayleigh numbers

With regard to the enthalpy profiles along the

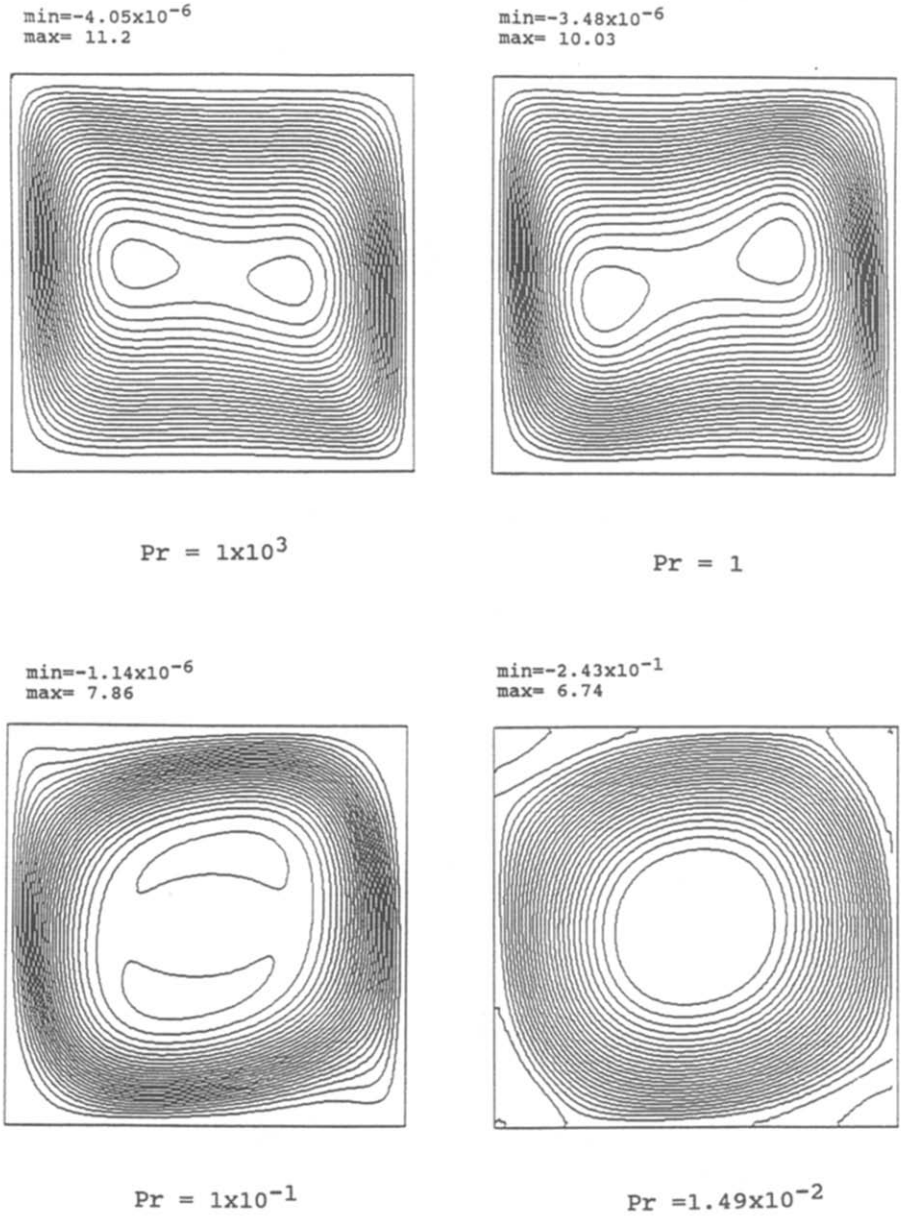

FIG 5 Effect of Prandtl numbers on streamfunction with $Ra = 10^5$ and no phase change

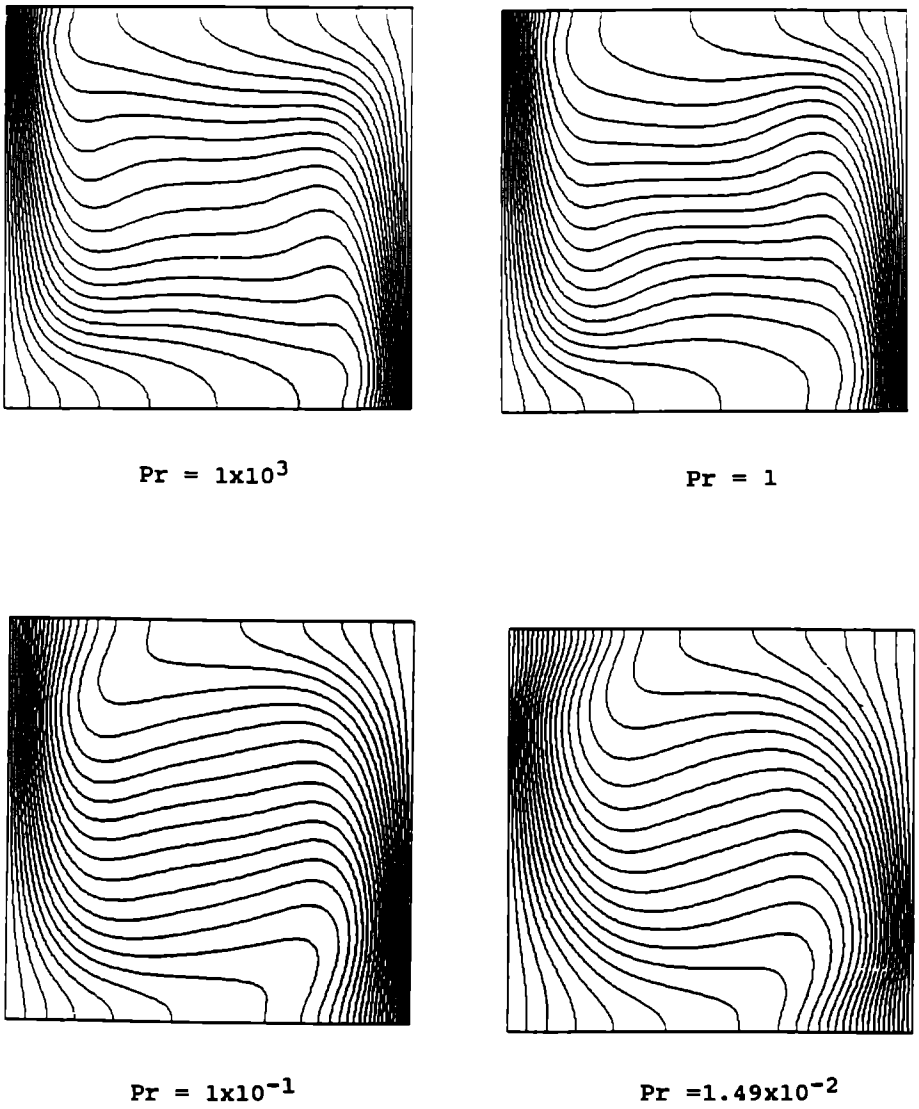

FIG 6 Effect of Prandtl numbers on enthalpy contours with $Ra = 10^5$ and no phase change

bottom wall, Fig. 7 shows that, compared to Fig 4 of $Ra = 10^4$, stronger convection induced by higher Rayleigh number causes sharper variations of the enthalpy profile for all Prandtl numbers; the quantitative differences among solutions are greater for $Ra = 10^5$ than for $Ra = 10^4$

The question may arise as with $Ra = 10^5$, whether the steady-state solutions exist for all Prandtl numbers? For example, it was found by Gresho and Upson [21] that with $Ra = 10^5$ and $Pr = 10^{-2}$, no steady-state solution can be obtained by their finite element formulation and modest spatial resolution (24×24 meshes) In the present study, we have found that although the convergences become progressively more difficult as Pr is reduced, stable steady-state solutions can be reached for all the cases reported here, especially when aided by the adaptive grid method

There have been many correlations proposed in the literature to relate the Nusselt number to Rayleigh and Prandtl numbers [14] A correlation proposed by Berkovsky and Polevikov [22] covers a very wide range of variations of Ra and Pr Without revealing much reasoning, Berkovsky and Polevikov gave the following correlation to link the Nusselt number, Nu, and the Rayleigh number as well as Prandtl number:

$$Nu = 0\ 18[Ra \cdot Pr/(0\ 2 + Pr)]^{0\ 29} \tag{5}$$

Earlier, Dropkin and Somerscales [23] reported a correlation based on a limited number of experimental measurements to include the effect of Pr

$$Nu = 0\ 069 Ra^{0\ 33}\ Pr^{0\ 074} \tag{6}$$

Equation (5) indicates that the impact of Pr on the heat transfer rate is negligibly small if $Pr > 1$. A larger effect of Pr on the heat transfer rate can be observed if $Pr < 1$. For example, with a fixed Ra, equation (5)

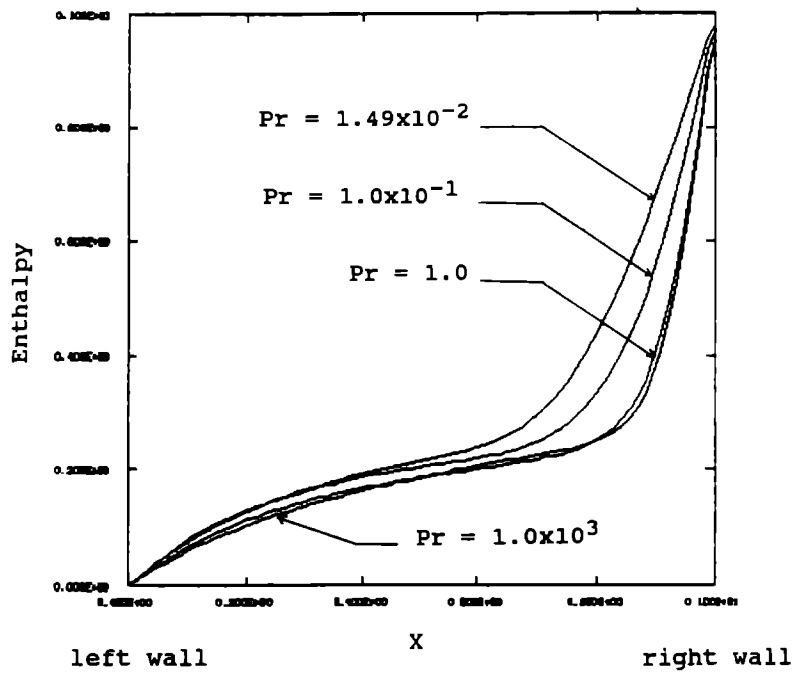

FIG. 7 Effect of Prandtl numbers on enthalpy profiles along bottom wall with $Ra = 10^5$ and no phase change

suggests that the relative changes of heat transfer rate from 10^3 to 1, 10^{-1}, and 1.49×10^{-2}, are, respectively, 5, 27, and 54%. For large Pr, equation (6) indicates a much stronger Prandtl number effect than equation (5) does. As pointed out by Gebhart *et al* (p 754 of ref [14]), the experiments by Dropkin and Somerscales [23] were not complete, small Ra was obtained only for small Pr and large Ra only for large Pr, thus giving a coupled Pr and Ra dependence of data

Our results agree qualitatively to equation (5) Figure 8 shows the Nusselt number vs Prandtl number with two different Rayleigh numbers based on the present solutions and equation (5) The Nusselt numbers shown in Fig 8 are computed based on the orig-

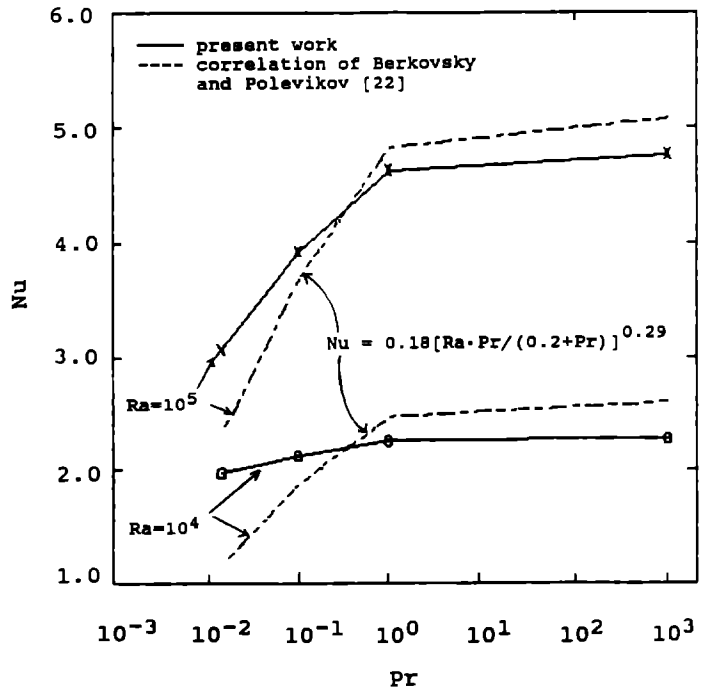

FIG 8 Nusselt number vs Prandtl number without phase change

inal definition

$$Nu = \bar{Q}/[\bar{K}(\bar{T}_H - \bar{T}_C)\bar{D}] \quad (7)$$

where $\bar{Q}$ is the heat transfer rate across any vertical surface, and $\bar{K}$ the thermal conductivity In terms of non-dimensional quantities, the following formula was adopted for computation on the left wall, based on the trapezoid rule:

$$Nu = \int_0^1 \left(\frac{\partial T}{\partial x}\right)\Big|_{x=0} \mathrm{d}y. \quad (8)$$

Figure 8 indicates that both equation (5) and our results show that the Nusselt number varies very little with large Pr; it changes more as Pr becomes less than one However, in our results the effect of Prandtl number on Nusselt number in terms of percentage variation becomes stronger as Ra increases. Equation (5), on the other hand, suggests that the relative effect of Pr on Nu remains the same for all Ra In the range of Ra that has been computed, the effect of Rayleigh number on the Nusselt number predicted by the present solution appears consistent with the results assembled by Kamotani *et al* [11] Caution should be exercised to extrapolate the present findings to even higher Ra, however, since it is shown in ref. [11] that the Rayleigh number effect on Nusselt number somewhat decreases as Ra goes beyond 10^5 There is a lack of definite information available in the literature to

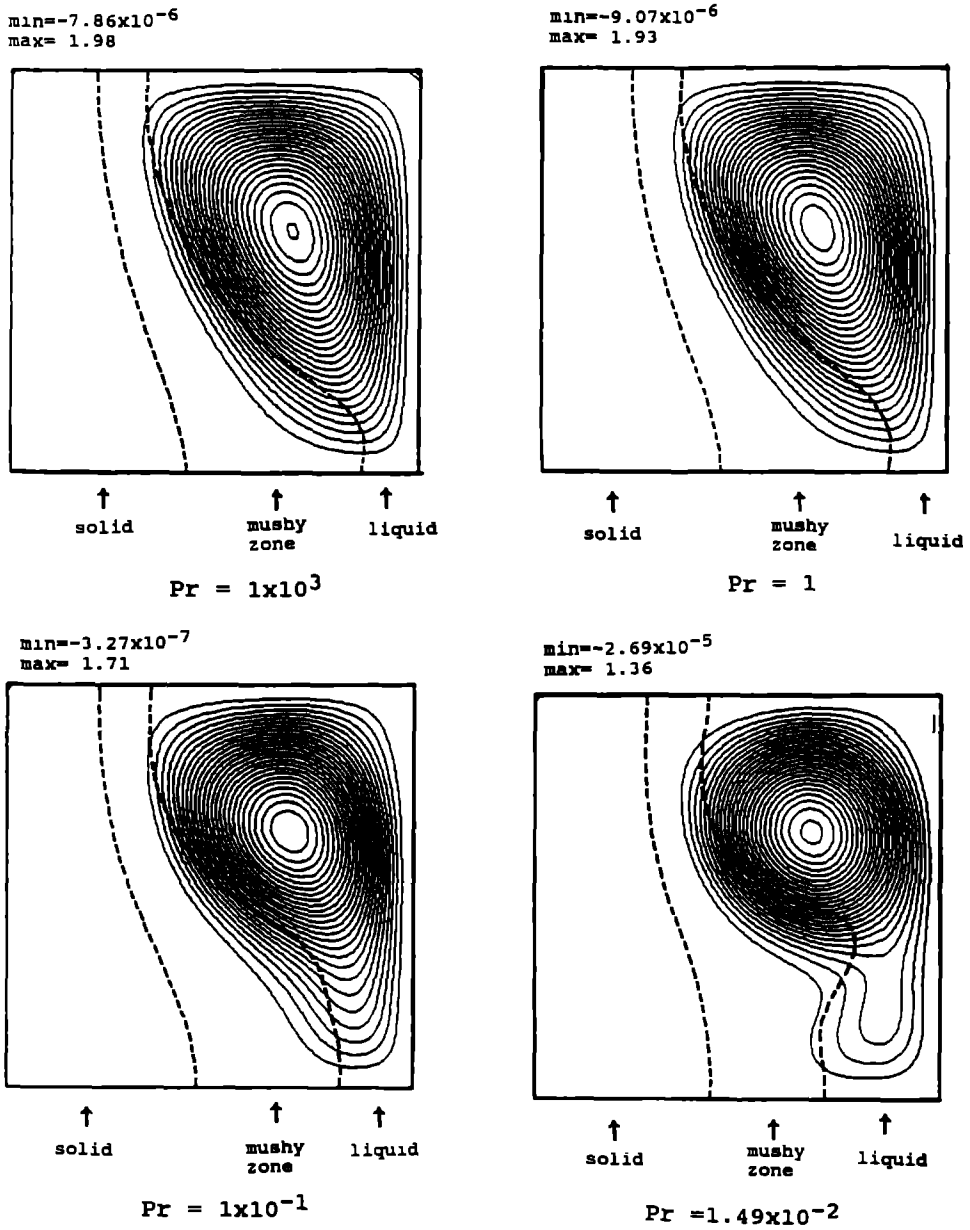

FIG 9 Effect of Prandtl numbers on streamfunction contours (solid lines) and phase boundaries (dotted lines) with $Ra = 10^4$ and with phase change

assess in detail the solutions presented here However, with appropriate interpolation, our solutions appear to agree very well, in terms of both the streamfunction and Nusselt number predictions, to several results reported earlier for $Pr = 0.71$ [19, 24–26]

3 2 *With solidification*

Next, we present the solutions of the transport process with the inclusion of solidification The Stefan number is chosen to be 0.2 in the present study Some streamfunction contours for cases with solidification have been presented in a previous paper [16] They are included here in different arrangements to aid our discussion We also refer to the information of enthalpy contours in ref [16]

3 2 1 $Ra = 10^4$ Figure 9 compares the streamfunction contours, along with the locations of liquidus, solidus, and mushy zones (shown in dotted lines) of the solutions with $Ra = 10^4$ and four different Prandtl numbers. Despite the obvious differences of convection pattern caused by solidification, the qualitative trend of the Pr effect appears the same as the single-phase cases. With respect to $Pr = 10^3$, the maximum convection strength decreases monotonically as Pr is lowered The decreases of the maximum streamfunctions are 2 5, 13 6, and 31 3%, for $Pr = 1$, 10^{-1}, and 1.49×10^{-2}, respectively Compared to the solutions without phase change (Fig. 2), the monotonic trend of convection strength vs Prandtl number remains unchanged The effect of Pr variation on convection strength is substantially more with solidification than without solidification in the low Pr regime, i e as $Pr < 1$ However, for the cases both with and without solidification, the relative effect of Pr on the solution is very limited with $Pr > 1$

The combination of Prandtl and Stefan numbers also makes the morphology of the mushy zone change substantially at $Ra = 10^4$ As Pr varies, not only does St exert a noticeable influence on the convection strength, but it changes the qualitative features related to the solidification process, including the shape of the phase boundary and the enthalpy distribution This difference in solution characteristics may not seem apparent based on the inspection of the wall temperature profile and heat transfer rate alone Figure 10 compares the bottom wall enthalpy profiles of four Prandtl numbers with solidification By comparing the wall enthalpy profiles with and without phase change, as shown in Figs 4 and 7, the changes of the characteristics of the wall temperature distribution caused by St are more pronounced than caused by Pr

3.2 2 $Ra = 10^5$ For the solutions with solidification under identical boundary conditions and Prandtl as well as Stefan numbers, but with $Ra = 10^5$, the corresponding solutions are shown in Figs 11 and 12. First, the higher Ra causes a stronger convection effect, making the convection cell penetrate deeper into the mushy zone as compared to $Ra = 10^4$ The enhanced convection results in both larger convection cells for all Prandtl numbers and more similar shapes among them A noticeable difference is for $Pr = 10^3$, where short wavelength wiggles are observed As discussed in ref [16], this feature does not appear to be caused by the numerical techniques adopted since these wiggles disappear with $Ra = 10^6$ where the nonlinear couplings among dependent variables are stronger and the numerical algorithm is expected to experience more difficulties in yielding convergent and accurate solutions

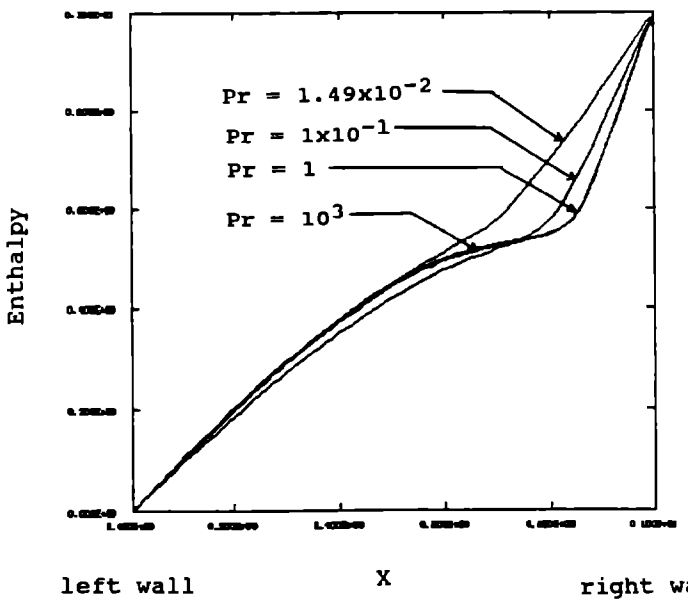

FIG 10 Effect of Prandtl numbers on enthalpy profiles along bottom wall with $Ra = 10^4$ and phase change

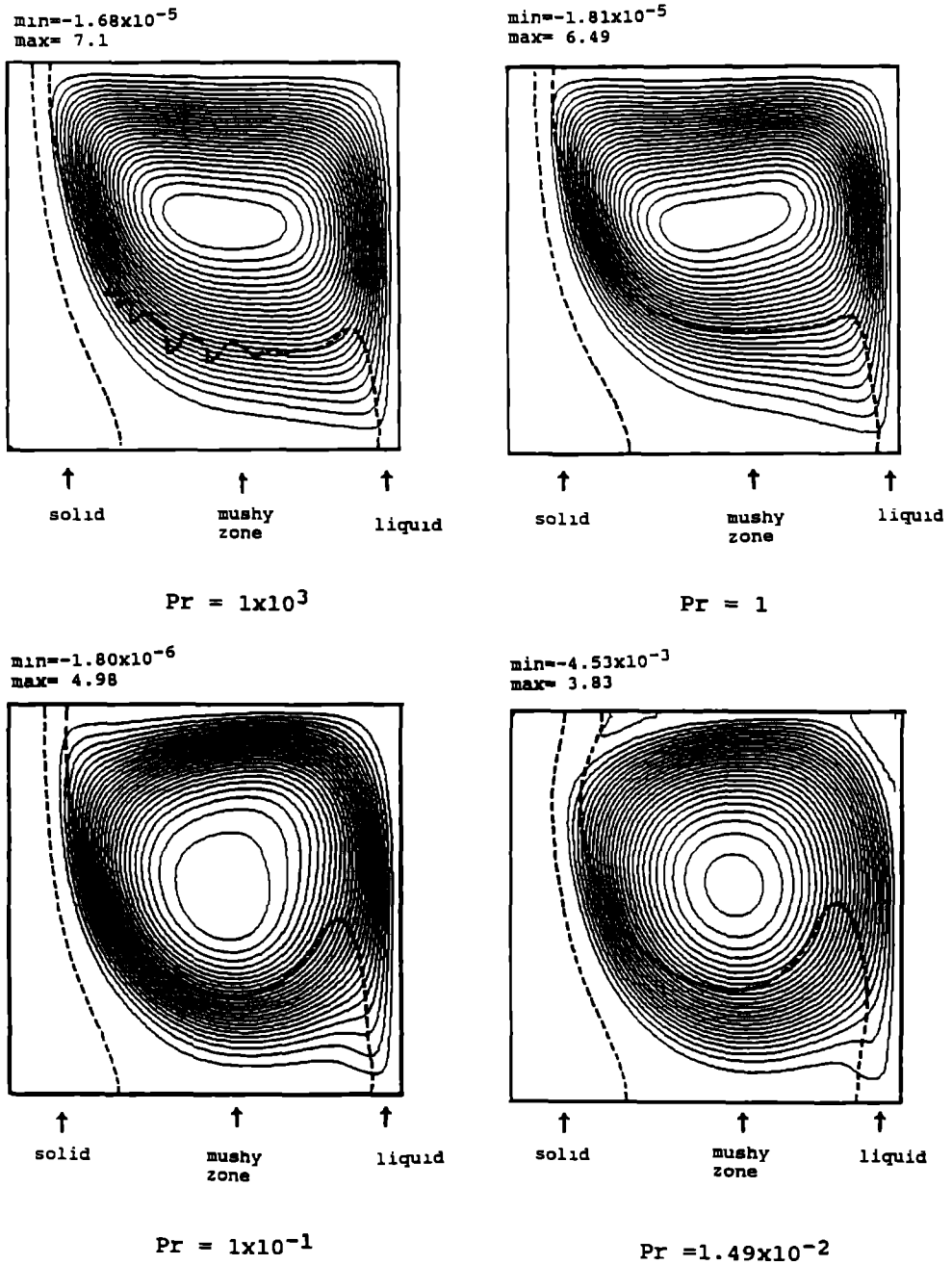

FIG 11 Effect of Prandtl numbers on streamfunction contours (solid lines) and phase boundaries (dotted lines) with $Ra = 10^5$ and phase change

It is interesting to note that, besides the wiggles of $Pr = 10^3$, the thermal fields with $Ra = 10^5$ as shown in the enthalpy contours in the whole domain [16], and enthalpy profiles along the bottom wall (Fig. 12), are of closer overall agreement among different Prandtl numbers than those with $Ra = 10^4$ (Figs. 9 and 10).

Figure 13 shows that Pr has a substantially larger effect on Nu at higher Ra Since Nu is calculated based on the integration of local gradients, it is the details of the temperature distribution rather than the overall characteristics that affect its value Figures 11–13 demonstrate that at $Ra = 10^5$ and with phase change, Pr variations can exert complicated influences on the thermal fields, causing the global pattern to be more similar while Nu to be more different For both $Ra = 10^4$ and 10^5, there are also substantial differences of phase boundary morphology between high and low Pr fluids

4. SUMMARY AND CONCLUSIONS

Based on the results presented, the following summary can be made

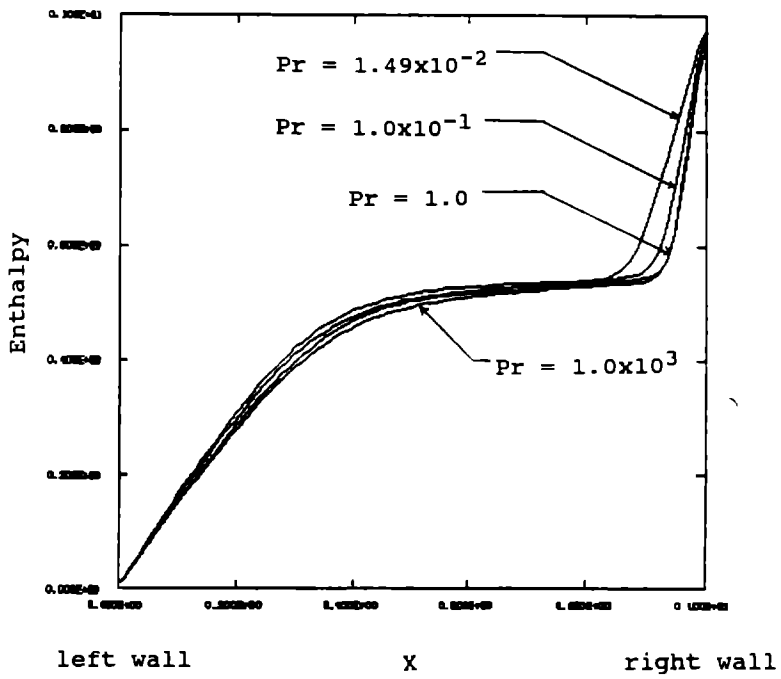

FIG 12 Effect of Prandtl numbers on enthalpy profiles along bottom wall with $Ra = 10^5$ and phase change

(1) With or without phase change, the transport characteristics are very insensitive to *Pr* when it is large The effect of *Pr* becomes more pronounced when it is lower than one

(2) As Rayleigh number increases, a stronger impact of Prandtl number on the convection strength can be seen, with or without solidification

(3) With regard to the thermal fields, as *Ra* increases, Prandtl number does not necessarily exert identical degrees of influence between single- and multiple-phase cases For single-phase cases, *Pr* effects on all aspects of the transport process increase with *Ra* With solidification, stronger convection at higher *Ra*, along with the Stefan number effects, result in larger

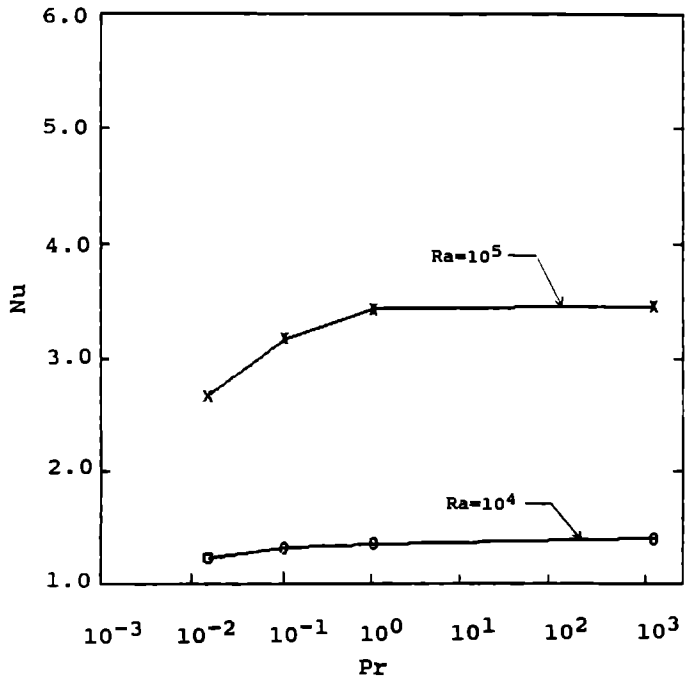

FIG 13 Nusselt number vs Prandtl number with phase change

Pr influences on maximum streamfunction and Nusselt number, but not on the global enthalpy pattern

(4) Overall, it is rather interesting that by varying *Pr* for five orders of magnitude, only modest differences in heat transfer rates and convection strength have been found in all cases, with or without phase change However, features such as morphology of phase boundaries may be more influenced than the transport characteristics are It is concluded that for the cases with solidification, care should be taken in deducing the information from materials of one Prandtl number to the other

The present studies are only limited to the steady-state solutions driven by the temperature field above There has been ample evidence that the variation of Prandtl number shows a substantial influence on the values of the transitional Rayleigh number from laminar to turbulent [14, 27]. It has also been clearly demonstrated that with the presence of double-diffusive convection of temperature and solute fields, the solutions of different Prandtl number can be different in qualitative patterns even with identical thermal and solutal Rayleigh number [20, 28, 29].

Acknowledgement—The authors are grateful to acknowledge the helpful discussion held with Drs D. Backman, Y Pang and D Wei of GE Aircraft Engines. Some of the computations were made using CRAY-XMP/48 of the National Center for Supercomputer Applications (NCSA) at the University of Illinois through a research grant

REFERENCES

1 R J McDonald and J D Hunt, Fluid motion through the partially solid regions of a casting and its importance in understanding a type segregation, *Trans Metall Soc. AIME* **245**, 1993–1997 (1969)
2 M C Flemings, *Solidification Processing* McGraw-Hill, New York (1974)
3 J Szekely and A S Jassal, An experimental and analytical study of the solidification of a binary dendritic system, *Metall Trans B* **9**, 389–398 (1978)
4 S Ostrach, Fluid mechanics in crystal growth, *ASME J Fluids Engng* **105**, 5–20 (1983).
5 M E Glicksman, S R Coriell and G B McFadden, Interaction of flows with the crystal–melt interface, *Ann Rev Fluid Mech* **18**, 307–335 (1986)
6 R A Brown, Theory of transport processes in single crystal growth from the melt, *A I Ch E Jl* **34**, 881–911 (1988)
7 C Beckermann and R Viskanta, Double-diffusive convection due to melting. *Int J. Heat Mass Transfer* **31**, 69–79 (1988)
8 C Beckermann, R Viskanta and S Ramadhyani, Natural convection in vertical enclosures containing simultaneous fluid and porous layers, *J Fluid Mech* **186**, 257–284 (1988)
9 W D Bennon and F P Incropera, A continuum model for momentum, heat and species transport in binary solid–liquid phase change system—II Application to solidification in a rectangular cavity, *Int. J Heat Mass Transfer* **30**, 2171–2187 (1987)
10 M E Thompson and J Szekely, Mathematical and physical modeling of double-diffusive convection of aqueous solution crystallizing at a vertical wall, *J Fluid Mech* **187**, 409–433 (1988)
11 Y Kamotani, L W Wang and S Ostrach, Experiments on natural convection heat transfer in low aspect ratio enclosure, *AIAA J* **21**, 290–294 (1983)
12 C Gau and R Viskanta, Effect of natural convection on solidification from above and melting from below of a pure metal, *Int J Heat Mass Transfer* **28**, 573–587 (1985)
13 T L Bergman and J R Keller, Combined buoyancy surface tension flow in liquid metals, *Numer Heat Transfer* **13**, 49–64 (1988)
14 B Gebhart, Y Jaluria, R L Mahajan and B Sammakia, *Buoyancy-induced Flows and Transport* Hemisphere, Washington, DC (1988)
15 J Crank, *Free and Moving Boundary Problems* Oxford University Press, Oxford (1984)
16 W Shyy and M -H Chen, Steady-state natural convection with phase change, *Int J Heat Mass Transfer* **33**, 2545–2563 (1990)
17 W Shyy, S S Tong and S M Correa, Numerical recirculating flow calculation using a body-fitted coordinate system, *Numer Heat Transfer* **8**, 99–113 (1985)
18 W Shyy, S W Correa and M E Braaten, Computation of flow in a gas turbine combustor, *Combust Sci Technol* **58**, 97–117 (1988)
19 W Shyy, Computation of complex fluid flows using an adaptive grid method, *Int J Numer Meth Fluids* **8**, 475–489 (1988)
20 W Shyy and M -H Chen, A study of transport process of buoyancy-induced and thermocapillary flow of molten alloy, AIAA Paper 90-0225, AIAA 28th Aerospace Sciences Meeting, Reno, Nevada, 8–11 January (1990)
21 P M Gresho and C D Upson, Application of a modified finite element method to the time-dependent thermal convection of a liquid metal In *Numerical Methods in Laminar and Turbulent Flow* (Edited by C Taylor, J A Johnson and W R Smith), pp 750–763 Pineridge Press, Swansea (1983)
22 B M Berkovsky and V. K. Polevikov, Numerical study of problems on high-intensive free convection In *Heat Transfer and Turbulent Buoyant Convection* (Edited by D. B Spalding and H Afgan), pp 443–455 Hemisphere, Washington, DC (1977)
23 D Dropkin and E Somerscales, Heat transfer by natural convection in liquids confined by two parallel plates which are inclined at various angles with respect to the horizontal, *ASME J Heat Transfer* **87**, 77–84 (1965)
24 G de Vahl Davis, Natural convection on air in a square cavity a benchmark numerical solution, *Int. J Numer Meth Fluids* **3**, 249–264 (1983)
25 N C Markatos and K A Pericleous, Laminar and turbulent natural convection in an enclosed cavity, *Int J Heat Mass Transfer* **27**, 755–772 (1984)
26 P LeQuere and T A de Roquefort, Computation of natural convection in two-dimensional cavity with Chebyshev polynomials, *J Comp Phys* **57**, 210–228 (1985)
27 P Chao, S W Churchill and H Ozoe, The dependence of critical Rayleigh number on the Prandtl number In *Convective Transport and Instability Phenomenon* (Edited by J Zierep and H Oertel), pp 55–70 Braun, Karlsruhe (1982)
28 B N Antar, Penetrative double diffusive convection effect of the Lewis and Prandtl numbers, *Int J Heat Mass Transfer* **31**, 895–898 (1988)
29 W Shyy and M -H Chen, Computation of double-diffusive convection with solidification in an enclosure, AIAA Paper 90-1721, AIAA/ASME 5th Joint Thermophysics and Heat Transfer Conf , Seattle, Washington, 18–20 June (1990)

EFFET DU NOMBRE DE PRANDTL SUR LES MECANISMES DE TRANSPORT INDUITS PAR LE FLOTTEMENT AVEC OU SANS SOLIDIFICATION

Résumé—Dans l'etude des mecanismes de transport avec solidification, quelques matériaux comme des solutions aqueuses qui ont de grands nombres de Prandtl (Pr) ont ete utilisés pour aider a comprendre les caracteristiques de la solidification de la silice ou des materiaux métalliques qui sont a faible Pr L'influence de Pr sur les phénomènes de transport induit par le flottement est etudiee a travers deux calculs pour l'écoulement bidimensionnel permanent, dans une cavite carree avec deux temperatures differentes des parois verticales, avec ou sans solidification Pour un nombre de Rayleigh constant (Ra), les caracteristiques des transports de la quantité de mouvement et de la chaleur sont insensibles a Pr si $Pr > 1$, que le changement de phase apparaisse ou non L effet de Pr devient plus sensible quand il tend progressivement vers un Pour les cas sans solidification, les effets de Pr sur tous les aspects du mécanisme de transport augmentent avec Ra Avec solidification, une convection plus vigoureuse induite par des Ra plus eleves et couplée avec les effets du nombre de Stefan conduit a une influence plus forte de Pr sur la fonction de courant maximale et sur le nombre de Nusselt, mais pas sur les configurations globales d'enthalpie On trouve aussi que la morphologie des frontieres des phases peut être plus sensible aux variations de Pr que le transport de quantite de mouvement et de chaleur

EINFLUSS DER PRANDTL-ZAHL AUF AUFTRIEBSBEDINGTE TRANSPORTVORGANGE MIT UND OHNE ERSTARRUNG

Zusammenfassung—Es werden die Transportvorgange bei der Erstarrung verschiedener Materialien von hoher Prandtl-Zahl (Pr)—wie z B waßrige Losung—untersucht Die gewonnenen Erkenntnisse werden dazu verwendet, das Erstarrungsverhalten von Silizium oder von metallhaltigen Materialien (kleine Prandtl-Zahl) verstehen zu lernen Der Einfluß der Prandtl-Zahl auf die auftriebsbedingten Transportvorgange wird durch zweidimensionale stationare Stromungsberechnungen in einem quadratischen Hohlraum bei zwei unterschiedlichen Temperaturen der senkrechten Wande mit und ohne Erstarrung untersucht Bei konstanter Rayleigh-Zahl (Ra) sind die Vorgange des Impuls- und Warmetransports fast unabhangig von der Prandtl-Zahl, wenn diese > 1 ist—dies gilt fur Falle mit und ohne Phasenanderung Der Einfluß der Prandtl-Zahl nimmt fur $Pr < 1$ zu Tritt keine Erstarrung auf, so nimmt der Einfluß der Prandtl-Zahl auf die Transportvorgange mit wachsender Rayleigh-Zahl zu Fur den Fall, daß es zu einer Erstarrung kommt, ergibt sich bei großerer Ra-Zahl eine starkere Konvektion, woraus sich—zusammen mit dem Einfluß der Stefan-Zahl—eine starkere Abhangigkeit der maximalen Stromfunktion und der Nusselt Zahl von der Prandtl-Zahl ergibt Daruberhinaus zeigt sich, daß Eigenschaften wie die Morphologie der Phasengrenze starker von der Pr-Zahl abhangen als der Impuls- und Warmetransport

ВЛИЯНИЕ ЧИСЛА ПРАНДТЛЯ НА ВЫЗААННЫЕ ПОДЪЕМНЫМИ СИЛАМИ ПРОЦЕССЫ ПЕРЕНОСА ПРИ НАЛИЧИИ И ОТСУТСТВИИ ЗАТВЕРДЕВАНИЯ

Аннотация—Для исследования характеристик затвердевания материалов на основе силикона или металлов с низким значением числа Pr использовались различные материалы (как, например, водные растворы), для которых характерны высокие значения числа Прандтля Pr Влияние числа Pr на вызванные подъемными силами явления исследуется посредством двумерных стационарных расчетов течения в квадратной полости для двух различных температур вертикальных стенок как при наличии, так и при отсутствии затвердевания. В случае постоянного числа Рэлея Ra характеристики переноса имнульса и тепла весьма незначительно зависят от числа Pr при $Pr > 1$ независимо от наличия фазового перехода. Эффект числа Pr становится более заметным при его монотонном убывании, начиная со значения единицы Что касается фазового перехода, то при отсутствии затвердевания влияние числа Pr на все характеристики процесса переноса увеличивается с ростом числа Ra. При налични затвердевания более интенсивная конвекция, обусловленная высокими числами Ra в сочетании с влиянием числа Стефана, приводит к усилению влияния числа Pr лишь на максимальную функцию тока и число Нуссельта, но не на общее распределение энтальпии Найдено также, что такие характерные свойства как морфология фазовых границ могут зависеть от изменений числа Pr в большей степени, чем перенос импульса и тепла